HHS Public Access

Author manuscript

Adv Funct Mater. Author manuscript; available in PMC 2015 August 17.

Published in final edited form as:

Adv Funct Mater. 2010 February 8; 20(3): 409–421. doi:10.1002/adfm.200901293.

Multifunctional Dendrimer-templated Antibody Presentation on Biosensor Surfaces for Improved Biomarker Detection

Dr. Hye Jung Han,
Department of Chemical Engineering and Materials Science, Wayne State University, Detroit, Michigan 48202 (U. S. A.) and Eunice Kennedy Shriver National Institute of Child Health and Human Development, NICHD, NIH, DHHS, Detroit, MI 48201 (U. S. A.)

Prof. Rangaramanujam M. Kannan,
Department of Chemical Engineering and Materials Science, Wayne State University, Detroit, Michigan 48202 (U. S. A.) and Eunice Kennedy Shriver National Institute of Child Health and Human Development, NICHD, NIH, DHHS, Detroit, MI 48201 (U. S. A.)

Sunxi Wang,
Department of Chemical Engineering and Materials Science, Wayne State University, Detroit, Michigan 48202 (U. S. A.)

Prof. Guangzhao Mao,
Department of Chemical Engineering and Materials Science, Wayne State University, Detroit, Michigan 48202 (U. S. A.)

Dr. Juan Pedro Kusanovic, and
Perinatology Research Branch NICHD/NIH/DHHS, Department of Obstetrics and Gynecology, Wayne State University, Hutzel Women's Hospital, Detroit, MI 48201 (U. S. A.)

Dr. Roberto Romero
Eunice Kennedy Shriver National Institute of Child Health and Human Development, NICHD, NIH, DHHS, Detroit, MI 48201 (U. S. A.)

Rangaramanujam M. Kannan: rkannan@chem1.eng.wayne.edu

Abstract

Dendrimers, with their well-defined globular shape and a high density of functional groups, are ideal nanoscale materials for templating sensor surfaces. This work exploits dendrimers as a versatile platform for capturing biomarkers with improved sensitivity and specificity. Synthesis, characterization, fabrication, and functional validation of the dendrimer-based assay platform are described. Bifunctional hydroxyl/thiol functionalized G4-polyamidoamine (PAMAM) dendrimer is synthesized and immobilized on to the polyethylene-glycol (PEG)-functionalized assay plate by coupling PEG-maleimide and dendrimer thiol groups. Simultaneously, part of the dendrimer thiol groups are converted to hydrazide functionalities. The resulting dendrimer-modified surface is coupled to the capture antibody in the Fc region of the oxidized antibody. This preserves the orientation flexibility of the antigen binding region (Fv) of the antibody. To validate the approach,

Correspondence to: Rangaramanujam M. Kannan, rkannan@chem1.eng.wayne.edu.

Supporting Information is available online from Wiley InterScience or from the author.

the fabricated plates are further used as a solid phase for developing a sandwich type ELISA to detect IL-6 and IL-1β, important biomarkers for early stages of chorioamnionitis. The dendrimer-modified plate provides assays with significantly enhanced sensitivity, lower nonspecific adsorption, and a detection limit of 0.13 pg ml^{-1} for IL-6 luminol detection and 1.15 pg ml^{-1} for IL-1β TMB detection, which are significantly better than those for the traditional ELISA. The assays were validated in human serum samples from normal (non-pregnant) woman and pregnant women with pyelonephritis. The specificity and the improved sensitivity of the dendrimer-based capture strategy could have significant implications for the detection of a wide range of cytokines and biomarkers since the capture strategy could be applied to multiplex microbead assays, conductometric immunosensors and field effect biosensors.

Keywords

biosensors; dendrimers; antibody conjugation; cytokine; Interleukin-6; IL-1β

1. Introduction

Advances in antibody-based diagnostics have focused on improving the specificity and sensitivity of immunoassay techniques. The specific molecular recognition of analytes and immobilized ligands at solid-liquid interfaces forms the basis for a large number of bioanalytical applications, including bio- and immunosensor diagnostic devices.[1] The solid-liquid interface results in sensitivity, and interaction at the analyte-ligand provides selectivity and stability. These parameters are strongly dependent of the receptor architectures, patterning, and of immobilization layer.[2] The key step in the development of immunosensors is the immobilization of antibodies onto a substrate at high density with uniform distribution, retaining their specific antigen-binding activities, and maintaining accessibility to the antigens.[3] Another important step is minimizing nonspecific adsorptions of extraneous cellular proteins on to the modified surfaces, which can reduce the sensitivity during detection steps. Dendrimers could play a vital role in each of these aspects.

Dendrimers are emerging as promising candidates for novel diagnostic platforms. Dendrimers can form stable, dense, well-organized, and close-packed arrays on substrate surfaces and ability to incorporate multiple branch ends available for consecutive conjugation reactions.[4] Fourth-generation amine-terminated polyamidoamine (G4 PAMAM-NH_2) dendrimers have a size similar to that of small proteins (i.e., streptavidin and G4 PAMAM-NH_2 dendrimer molecules are both in the range 4-5 nm).[5] In addition, dendrimers can have a larger area of capture than linear analogs with consequently high capture probability. Dendrimers have been utilized in dip-pen nanolithography,[6] DNA and protein arrays,[7] nanocatalyst-based electrochemical immunosensor,[8] biosensor-based on dendrimer encapsulated Pt nanoparticles[9] and regenerable affinity biosensing surfaces.[10] Recent work on a glass surface coated with a polyamidoamine dendrimer terminated with carboxylic acid group (PAMAM-COOH), showed that the dendrimer-modified surface had relatively low nonspecific cellular protein adsorption, and can also enable antibody binding.[3a]

The kinetic and equilibrium binding analyses of streptavidin-biotin interactions on biotinylated PAMAM-NH_2 dendrimer monolayers showed that the initial binding rate of streptavidin (SA) up to the saturation level was 2-fold higher in all dendrimer layers than in the other tested systems of 11-mercaptoundecylamine SAMs and a poly(L-lysine) layer regardless of the surface density of functionalized biotin.[11] Concurrently, the dendrimer layers led to much higher values of sticking probability[12] and prolonged the significant levels around the maximum probability with increasing SA coverage. It was suggested that faster binding of SA and highly ordered packing of the molecules seems to originate from typical properties of the dendrimer monolayers, such as surface distribution of functionalized biotin, surface corrugation, and flexibility of highly branched larger dendrimers which suggest a guideline for the construction and analysis of an interfacial layer in biosensing application. However, nonspecific adsorption by avidin on to the G4 PAMAM-NH_2 monolayers was observed to be about 12% relative to the specific avidin binding.[13] This finding might limit the use of amine-terminated G4 PAMAM-NH_2 dendrimer monolayers as a biomolecular interface.

These studies suggest that, in general, two functionalities are needed for successful construction of diagnostic interfaces: (i) a bio-active surface to immobilize antibodies and (ii) a bio-inert one to minimize nonspecific absorption of protein that results in a poor signal-to-noise ratio.[14] A number of strategies have been attempted to minimize nonspecific protein adsorption on a solid surface,[15] even though the mechanism of protein adsorption onto a chemically modified surface remains to be elucidated. PEG and oligo(ethylene glycol) (OEG) are well known biomaterials to reduce nonspecific protein adsorption on a variety of surfaces, mainly due to steric repulsion and excluded-volume effects.[16] Based on the previous findings, this study uses a neutral G4-PAMAM dendrimer.

Intra-amniotic infection/inflammation (IAI) is one of the most important mechanisms of disease in preterm birth. Preterm birth is a major problem in modern perinatal medicine and accounts for 75% of the perinatal mortality and 50% of the perinatal morbidity.[17] The association between IAI and preterm labor and birth has been well established.[18] However, IAI is often *subclinical* with signs such as fever, uterine tenderness and fetal tachycardia, which usually occur late and are present in only a small portion (12.5 %) of women with microbiologic evidence of infection.[19] Interestingly, pro-inflammatory cytokines such as IL-1β, IL-6, MMP-8 and TNF-α have been found in high concentrations in the amniotic fluid of women with preterm labor and intra-amniotic fluid infection[20] and an elevated concentration of pro-inflammatory cytokines in amniotic fluid is a sensitive and powerful predictor of IAI.[21] To prevent fetal damage and to facilitate the development of novel treatments, there is an urgent need to develop a highly sensitive and specific diagnostic device for the early detection of pro-inflammatory cytokines and novel biomarkers for IAI.

Interleukin-6 (IL-6), a pleiotropic cytokine that has a critical role in the inflammatory response, has been implicated in the pathogenesis of a number of inflammatory conditions, such as psoriasis, inflammatory arthritis, cardiovascular disease, and inflammatory bowel disease.[22] IL-1β is an important mediator of the inflammatory response, and is involved in a variety of cellular activities, including cell proliferation, differentiation, and apoptosis. IL-6 is one of the most used markers of IAI in different studies and fetal inflammatory

response syndrome is operationally defined as a fetal plasma IL-6 concentration above 11 pg ml^{-1}.[23] IL-6 is also clearly linked to the outcome of the child and can predict delivery within 7 days.[17a] Therefore, early and sensitive detection is a key for diagnosis of IAI and the determination of IL-6 and IL-1β levels are very useful for clinical diagnosis of IAI.

In this paper we describe synthesis, characterization, fabrication and functional evaluation of a *neutral* G4-PAMAM-OH-based biosensing platform for IL-6 and IL-1β detection, using a multi-step synthesis involving modification and functionalization of the polystyrene plate. Studies on the interaction between PAMAM dendrimers with different surface groups (-COOH, $-NH_2$, -OH) and proteins revealed that G4-PAMAM-OH dendrimers showed minimal interactions with proteins.[24] Hydroxyl functionalized PAMAM dendrimer was expected to be more effective in reducing nonspecific adsorption of proteins, while retaining the unique structural features of the dendrimer molecule. To improve the nonfouling character of the surface, we constructed mixed PEG tethered chains on the plate surface by co-immobilization of appropriately chosen heterobifunctional PEGs. Since the PEG group also has hydrophilic property, it can improve the hydrophilicity of the sensor surface. Given that antigen-antibody immunoreactions take place in aqueous phase, reactivity between the immobilized antibody and antigen is also expected to improve. PEG-maleimide groups were used to immobilize dendrimers. In this way, we introduce dendrimer after the PEG monolayer has been assembled and control dendrimer grafting density which ultimately reflect antibody grafting density. Relatively long 3.4k PEG and dendrimer gives diffusional and conformational flexibility, which gives more favorable antibody-antigen interactions. Modified surfaces morphology was examined by atomic force microscopy. The resulting dendrimer functionalized surfaces were employed as templates to immobilize anti-human IL-6 and IL-1β antibody and the performance was evaluated by the detection of IL-6 and IL-1β using sandwich format ELISA. The dendrimer-based assay was compared to commercially available IL-6 and IL-1β ELISA kit, and validated in human serum samples.

2. Result and Discussion

2.1. Synthesis of hydroxyl/LC-PDP functionalized G4-PAMAM dendrimer

In order to reduce the nonspecific protein adsorption, amine-terminated G4-PAMAM dendrimers were surface-modified with isothiocyantobutanol **1** and linker succinimidyl 6-(3'-[2-pyridyldithio]propionamido)hexanoate (LC-SPDP) for dendrimer immobilization and antibody conjugation (Scheme 1). In designing a hydroxyl/6-(3'-[2-pyridyldithio]propionamido)hexanoate (LC-PDP) functionalized dendrimer, we utilized the amide and thiourea linkages which are stable for subsequent reactions. First, G4-PAMAM dendrimer was conjugated with heterobifunctional cross-linking agent LC-SPDP through a stable amide bond to provide a protected thiol in the form of a disulfide bond. The number of conjugated LC-PDP linkers was determined by UV spectroscopy, using the pyridine-2-thione assay and MALDI-MS (Supporting Information Figure S4 and S5). On the basis of these analyses, an average of thirteen disulfide groups per dendrimer in **2** was estimated (for detailed procedures, please see experimental section). Remaining amino groups of **2** (~ 46) were converted to hydroxyl group by reacting with isothiocyantobutanol **1** through stable thiourea linkage to give hydroxyl/LC-PDP conjugated G4-PAMAM **3**. The disulfide bond of

LC-PDP linker was reduced by tris(2-carboxyethyl) phosphine (TCEP) to thiol groups quantitatively.[25] The resulting conjugate **4** was used *in situ* for subsequent reaction without purification. Parts of thiol groups in dendrimer **4** were conjugated to maleimide groups of PEG-modified plate to immobilized dendrimer and remaining free thiol groups were conjugated hetero-bifunctional cross linker *N*-(ε-maleimidocarproic acid)hydrazide (EMCH) which were used to capture the antibody. In order to test the efficiency of the thiol-maleimide conjugation reaction, a model reaction was performed. Thus, all the thiol groups in dendrimer **4** were conjugated with EMCH to give hydrazide functionalized dendrimer **5**. This thiol-maleimide conjugation reaction was carried out at 4°C to prevent possible side reaction, since a condensation reaction of thiourea and maleimides at high temperature was reported (at 40°C, 14 h reaction time, 50 % conversion to 2-iminothiazolidin-4-one).[26] The integrity of this reaction was confirmed by ^{1}H NMR of dendrimer **5**, which shows characteristic succinimide ring methine proton α to sulfur at 3.9 ppm [SC***H***(C=O)CH_2, dd, *J* = 12 and 4.8 Hz] and no condensation product 2-iminothiazolidin-4-one methine proton which typically appears at above 4.5 ppm. ^{1}H NMR of dendrimer **5** also shows hydrazide amide proton, N***H***NH_2(C=O), at 8.9 ppm (Figure S9). Conjugate **2, 3**, and **5** were characterized by ^{1}H NMR, MALDI-MS, UV -Vis and HPLC (Figure S1-S11).

2.2. Surface modification with PEG and dendrimer immobilization

In order to reduce nonspecific protein adsorption, polyethylene glycol was tethered to the carboxylic acid functionalized 96 well polystyrene plates (Corning® high bind plate). It has been proposed that the protein resistance of the self-assembled mono layers (SAMs) derived from PEG is related to the conformation, chain length, mobility (flexibility), and surface density of PEG chains.[27] The nonspecific adsorption of proteins on the surface decrease with the increasing molecular weight of PEG chain. However, the tethered chain density decreases with increasing PEG molecular weight due to the exclusion volume of each chain on the surface. Thus, the PEG tethered chain density and its molecular weight has a trade-off relation.[28] We co-immobilized amine functionalized PEG-maleimide (NH_2-PEG-Mal, MW 3.4k Da) and PEG-hydroxyl (NH_2-PEG-OH, MW 2k Da) to improve the nonfouling character of the surface and also cover the 'defects' on the polystyrene plate.[29] NH_2-PEG-Mal groups were used for immobilization of dendrimer. Therefore, NH_2-PEG-Mal grafting density reflects the dendrimer graft density on the surface. The appropriate dendrimer grafting density was estimated by considering the characteristic sizes of dendrimer diameter (~5 nm), antigen (IL-6 and IL-1β) diameter (4~5 nm, MW 17~22k Da.) and antibody dimension (14.5 nm long × 8.5 nm wide × 4 nm thick).[30] We assumed that the dendrimers would form a hexagonally close packed monolayer on the surface (Figure S12). The minimal packing area (upright position) of IgG is 34 nm^2 and maximal packing area (lying position) is 123 nm^2. In order to reduce the steric hindrance between antibody-antigen interactions,[31] we placed one dendrimer (antibody) at the center of every hexagon, and the rest of the space was filled with NH_2-PEG-OH. The calculated area of hexagon unit cell is 65nm^2, which is roughly the average of minimal and maximal packing areas of IgG.

Reaction conditions for the functionalization of polystyrene plate with PEG were chosen to minimize ring opening side reaction. Carboxylic acid groups of polystyrene plate were activated by EDC and 1-hydroxybenzotriazole hydrate (HOBT) (Scheme 2). The resulting

HOBT activated carboxylic groups could be hydrolyzed under desired mild conditions which minimized the ring-opening side reaction of the NH_2-PEG-Mal.[32] Although no significant ring opening was observed at pH values up to 7.0, reactions were conducted at pH 6.5 that minimized ring opening and maximized nucleophilicity. Two equivalents of NH_2-PEG-Mal were reacted, based on the calculated dendrimer grafting density, considering the yield of the amidation reaction and the reduced reactivity of thiol-maleimide conjugation reaction in the presence of TCEP.[25b]

For good protein repulsion, high grafting densities of end-functionalized linear PEG chains are required. For chemisorption of end-functionalized linear PEG, the highest surface coverage can be obtained when the grafting solution provides marginal solvation conditions (cloud point), where the chain repulsion between PEG chains during the grafting process is reduced, thus increasing their grafting density. The critical concentration marking the overlap of PEG chains in solution, C_{crit} depends on both the molecular weight of the PEG and its radius of gyration.[33]

$$C_{crit} = \frac{M}{N_A \frac{4}{3}\pi R_G^3} \quad (1)$$

For 2k PEG, the radius of gyration in aqueous solution was reported as 18 Å,[34] and critical concentration was calculated as 40 mg per 300 μl (per well volume). Various grafting densities of NH_2-PEG-OH (10, 20, 30 and 40 mg) were tested. However no significant difference in sensitivity, detection limit and the background in the assay outcome were observed. The background intensity at each of the PEG grafting densities was nearly identical (~0.025 O.D.) and low. These values are comparable to the background of optimized ELISA kit. This suggest that the reaction between the surface carboxyl groups and the NH_2-PEG-OH was effective, and appropriate PEG coverage was attained with 10 mg grafting density. This was further analyzed using atomic force microscopy.

Dendrimer immobilization was carried out inside the glove bag under the constant flow of nitrogen at 4°C, and unreacted maleimide groups were further reacted with 2-thioethanol. To test dendrimer immobilization and EMCH conjugation, thiol/hydroxyl functionalized G4-PAMAM **4** and a fluorescence analogue 1-(2-maleimidylethyl)-4-(5-(4-methoxyphenyl)oxazol-2-yl)pyridinium methanesulfonate (PyMPO-maleimide) (*instead of EMCH*) were immobilized onto the PEG-modified ELISA plate under the same reaction conditions (Scheme S1). Thus, a series of different concentrations of NH_2-PEG-Mal (14.8, 29.6 and 44.4 pmole) immobilized ELISA plate was prepared and different concentrations of dendrimer **4** (5.9, 11.8 and 17.7 pmole) was reacted respectively. To this, 15 equivalent of PyMPO-maleimide to each dendrimer concentration was reacted and fluorescence intensity was measured. As dendrimer concentration increases, PyMPO fluorescence intensity also linearly increases suggesting that dendrimer and EMCH immobilization is successful and the reaction ratio of dendrimer to PEG-Mal and EMCH is relatively constant within a range of tested concentration (Figure 1). The dendrimer modified plates were stored at -20 °C and stable for several months with no signs of reduced reactivity, suggesting that the dendrimer-modified plates are stable and have an appreciable life time.

2.3. Antibody immobilization onto polystyrene plate

The sensitivity of an immunosensor for the detection of antigens with a very low concentration can be increased by control of the orientation of antibodies immobilized on the sensor surface and with decreasing the steric-hindrance effect. When antibodies are immobilized on a solid-phase surface, their binding activity is usually less than that of soluble antibodies.[35] This reduction of binding activity is due to a combination of steric-hindrance, denaturation of proteins and random orientation.[36] Thus, the development of the immobilization method for antibodies which provides favorable antigen binding orientation is highly desirable.

A variety of techniques are currently available for immobilizing antibodies on assay surfaces. These include covalent coupling using amines on lysine residues of antibody, or orientated immobilization by using an intermediate protein that binds to the Fc region of antibodies.[37, 38] However, those methods have some drawbacks such as lose binding activity due to direct chemical modification of the antigen binding site[39] or lower surface density of immobilized antibody since two immobilization steps are required. Other methods are chemically modifying the carbohydrate on the Fc region of antibody and selectively reducing disulfide bond of cysteine residue in the hinge region of antibody. Both of these methods can increase the fraction of active antibody fragments.[40]

Antibodies are glycoproteins containing 3-12% carbohydrates at conserved N-glycosylation sites located in CH2 domains of the Fc portion at Asn-297.[41] Glycosylation of these sites seems to have little, if any, effect on antigen binding. The Asn-linked oligosaccharide of IgG is known as a biantennary, complex type glycoforms.[42] In addition to the conserved glycosylation sites in the Fc, the variable (Fv) domain is glycosylated in approximately 20% of IgGs.[43] However, their frequency and location are dependent upon the occurrence of Asn-Xaa-Ser(Thr) sites in the hypervariable region where X can be any amino acid except Pro or Glu.[44] O-linked oligosaccharides have also been reported mostly located in the hinge region or possibly on Fc region.[45]

Mouse anti-human IL-6 and IL-1β antibodies were immobilized by their oligosaccharide moieties to dendrimer hydrazide linker. To immobilize antibody, carbohydrate vicinal hydroxyl groups in the Fc region of antibody were oxidized by sodium periodate in PBS buffer (pH 7) to aldehyde (Scheme 3). Studies on the rate and immunoreactivity of antibody oxidation by periodate have shown that the number of oxidized sites generated by $NaIO_4$ depends on pH, temperature, reaction time and the concentration of the oxidizing reagent.[46] Building on the previous results, we examined the degree of antibody oxidation over 80 minutes at periodate concentrations between 0.47 and 3.7 mM by aldehyde-modifying reagent Purpald® (Aldrich) with formaldehyde as a calibrator (Figure S13).[47] To preserve the immunoreactivity of the antibody, we employed a mild oxidation condition: 1mg of antibody in PBS pH 7 was oxidized by treatment with 0.1 mg $NaIO_4$ (0.47 mM) for 15 min. at 4°C in the dark. Under these conditions, approximately 8 aldehyde groups per antibody were produced according to Purpald test (Figure S14). The resulting oxidized antibody was quickly separated from the oxidizing reagent by the Amicon® centrifugal filter device and the gel filtration with concomitant buffer exchange, and was allowed to react with the dendrimer in phosphate buffer at pH 8, 4°C for 3 h. The reaction of the dendrimer

hydrazide end group with antibody aldehyde group formed hydrazone linkage. Since this Schiff base is unstable,[48] *in situ* reductive amination with sodium cyanoborohydride gave stable secondary amine linkage. In the literature, this step is commonly run at a pH value above 9 but some degradation of PAMAM dendrimers has been observed at pH 9 over prolonged periods. Further, the immunoreactivity of antibody precludes the use of these conditions.[49] At the end of the reaction, ethanolamine was added to block reaction of the remaining aldehyde groups. The amount of immobilized antibody was estimated to 418 ng/well by bicinchoninic acid (BCA) protein assay of supernatant of reaction solution and about 0.7 antibody molecule per hexagonal unit cell (65 nm^2) were immobilized.

To monitor and validate the antibody-dendrimer conjugate reaction on the plate, a model reaction was carried out. Hydrazide and PyMPO (fluorescence tag)-functionalized dendrimer **6** was synthesized, and the conjugation reaction with the oxidized antibody was performed at the *same* reaction conditions (Scheme S2). The reaction mixture was qualitatively analyzed by immuno-precipitation (IP) using IgG-binding proteinG-immobilized agarose gel. The fluorescence spectra of free hydrazide/PyMPO functionalized dendrimer **6** showed maximum emission intensity 1985 units at 570 nm (Figure 2A), as expected. The dendrimer **6** was incubated with proteinG-immobilized agarose gel and separated by spin filter. The flow-through free dendrimer **6** solution showed a reduced fluorescence intensity (59 RFU, Figure 2C), suggesting that a small amount of free dendrimer **6** was nonspecifically adsorbed to the gel. This nonspecifically adsorbed dendrimer **6** was further eluted by adding elution buffer and fluorescence intensity was measured (46 RFU, Figure 2F). From the fluorescence intensity, degree of nonspecific adsorption of free hydrazide/PyMPO-functionalized dendrimer **6** was estimated to be about 3%. The reaction mixture of antibody-dendrimer conjugation reaction, which contains free antibody, free hydrazide/PyMPO-functionalized dendrimer **6** and the antibody-dendrimer **6** conjugate showed a max fluorescence 1994 RFU (Figure 2B). After IP, the flow-through reaction mixture showed a reduced fluorescence intensity (343 RFU, Figure 2D). The reduced fluorescence intensity is due to complex formation between antibody-dendrimer conjugate **6** and protein G, and nonspecific adsorption of free dendrimer **6** to the gel, since free antibody showed no emission (Figure 2G). The bound antibody-dendrimer conjugate, antibody and dendrimer **6** were eluted by adding elution buffer and fluorescence spectra of *eluted* solution showed max fluorescence intensity 331 RFU (Figure 2E). Therefore, approximately 321 RFU comes from the antibody-dendrimer conjugate since about 3% of emission is due to nonspecifically bound free dendrimer **6**. Therefore it was estimated that about 17% of hydrazide/PyMPO-functionalized dendrimer **6** were reacted with antibody. Since the dendrimer-antibody conjugation reaction on the plate was performed under similar conditions, it is expected to be successful.

2.4. Morphology of the dendrimer-antibody modified plate

To characterize the molecular arrangement on the modified surface, we imaged the surface using AFM. Figure 3a is an AFM height image of 2k PEG-OH and 3.4k PEG-Mal modified ELISA plate (in air). The modified surface is fully covered by PEG and displays smooth and uniform surface features over the micrometer range. This suggests that the PEGlyation

reaction conditions were appropriate. The surface roughness (R_q) of the PEG-modified surface was found to be 0.6 nm for 550 × 550 nm^2 images as represented by Figure 3a.

Figure 3b is an AFM height image of the dendrimer **4** attached to the PEG-modified ELISA plate. From the sectional analysis, the dendrimers were estimated to have a size range of 9.5-11.5 nm in lateral diameter and 3 ± 0.5 nm in height. The apparent lateral diameter measured by AFM is larger than the predicted diameter value of 4.5 nm for a spherical G4 PAMAM dendrimer molecule. The difference between vertical and lateral sizes can be caused by adsorption, drying, and tip convolution.[50] This image is consistent with previously published data[51] it however has features, which is similar to those observed on the PEG substrate, making the discrimination of features related to either types of surface difficult. There also exist some larger features on the modified surface as the one in red circle in Figure 3b, which has a dimension of 60.5 nm × 5.5 nm (lateral diameter and height, respectively). These particles are likely to be the aggregated dendrimers (perhaps two molecules). The bearing area analysis gives the percentage of the surface above the chosen reference plane. The estimated surface coverage of the dendrimer is around 1%, which is consistent with the features shown Figure 3c (image of dendrimer-antibody conjugate on the PEG surface by AFM) on this dendrimer modified substrate.

Figure 3c is an AFM height image for antibody-dendrimer conjugate attached on PEG modified substrate in PBS buffer. There are mainly two kinds of features in the circles with different colors. Red ones have a size range of 30-40 nm in lateral diameter and 7-10 nm in height, green ones have a size range of about 15 nm in lateral diameter and 2-4 nm in height. The red ones are consistent with the antibody-dendrimer conjugates and the green ones are consistent with the dendrimers. The height increase is the result of antibody-dendrimer conjugation and is consistent with the antibody dimension (14.5 nm × 8.5 nm × 4 nm). About 15-20 antibody-dendrimer conjugates were found in a area of 500 × 500 nm^2, or one antibody per 100 × 100 nm^2. There are relatively few objects with the Y-shape morphology of the IgG antibodies in the image (e.g., the one in the blue circle). This could be due to the antibody being orientated perpendicular to the substrate as desired for biosensing applications. Antibodies are expected to have more upright position on the dendrimer surface exposing their antigen binding site to the solution phase since it is covalently attached to dendrimer using its oligosaccharide moiety at the Fc portion, therefore showing more globular-like features as in the red circles.

2.5. ELISA evaluation of dendrimer-modified surface

To evaluate the diagnostic performance of the dendrimer-based assay, recombinant human IL-6 and IL-1β were assayed by the sandwich ELISA format using biotinylated goat anti-human IL-6 and IL-1β as detection antibodyies and streptavidin-HRP as a reporter. Two different substrate tetramethylbenzidine (TMB) and luminol were employed. Various known standard concentrations of IL-6 in the range of 0-300 pg ml^{-1} (0-250 pg ml^{-1} for IL-1β) were assayed and typical dose-response curve was acquired. The reaction time between antibodies on the sensor and the cytokines was 2 h, and was the same as that for the kit plate. These data were compared with commercially available IL-6 and IL-1β ELISA kit, and anti human IL-6 and IL-1β capture antibody coated plate by physical adsorption (Figure 4).

The linear regression equation for dendrimer plate for IL-6 was $A = 0.0425 + 0.0065*C_{[IL-6]}$, with the linear regression coefficient R = 0.9998. The lower limit of detection (LLD, 3STD) of IL-6 was determined to be 0.29 pg ml^{-1} for TMB detection and 0.13 pg ml^{-1} for luminol detection (Table 1). In literature, various methods have been developed for determination of IL-6 levels, such as microfluidic immunosensor,[22a] conductometric immunosensor,[8b] microsphere-based immunoassay[52] and capacitive biosensor[53] with varying detection limits. Dendrimer based assay in present study has a detection limit superior to that of other previously reported IL-6 assay except that obtained by Johansson *et al*. using potentiostatic capacitance measurements.[53] Dendrimer modified plate showed 3 fold improvement on the detection limit compare to kit plate for TMB detection (0.29 pg ml^{-1} vs. 0.89 pg ml^{-1}) and 7 fold improvement for luminol detection (0.13 pg ml^{-1} vs. 0.89 pg ml^{-1}). Even though less antibodies were immobilized on to the dendrimer plate compare to that by physical adsorption (418 ng vs. 758 ng per well), the dendrimer plate showed significant improvement in detection limit (0.29 pg ml^{-1} vs. 5.75 pg ml^{-1}). This suggests that the dendrimer-based capture strategy is 20 fold better than the scientific control (physical adsorption). These results also suggest that the proposed strategy for preventing non-specific adsorption using hydroxyl functionalized dendrimer and PEG is effective (compare O.D. of zero replicates of dendrimer plate 0.034 vs. 0.319 for physical adsorption) and dendrimer conjugation reactions to the antibody preserved the activity of the antibody. The dendrimer-based assay also performed better than the commercially available ELISA kit for IL-6.

The sensitivity (*S*) is defined as the slope of the regression line of the signal versus concentration plot. For dendrimer modified plate and kit plate, *S* values were 0.0065 and 0.0054 Abs/pg ml^{-1} respectively. The difference in the slope of the dose-response curve can be explained by the enhanced binding efficiency of the antibodies immobilized on the dendrimer compare to kit plate. The steeper slope also suggests that more powerful signal amplification method could further improve the detection limit, which we demonstrate by luminol detection.

To evaluate overall *specificity* of the designed immunosensors, the potential interference toward IL-6 detection from co-existing cytokine species was studied with the dendrimer modified ELISA plate. Using a standard solution containing each 300 pg ml^{-1} of IL-1β, TNF-α and IL-6, the selectivity of the proposed immunosensor was examined by ELISA. No significant difference of O.D. was observed in comparison with the result obtained in the presence of only IL-6.

The dendrimer plate had good precision with relative standard deviation (R.S.D) 10.1% of the five zero standard replicates. The intra-assay variability was determined by calculating the CV between the duplicates within each run, for each dilution concentration. The obtained values ranged between 1.2 and 11.4% in each of 5 independently run assays. The inter-assay variability was determined by calculating the CV between values obtained in 5 independent assay runs. The obtained CVs ranged between 2.1 and 7.5%. This indicated that assay is reproducible considering that, in the case of immunoassays such as ELISA, it is generally accepted that intra- or inter-assay variability should be lower that 10 – 15% for the

assay to considered precise enough for its use and differences in quality between different batches of manually-coated plate.

In order to assess the accuracy and applicability of the present method in a clinical setting, human serum samples (from normal non-pregnant woman) were spiked with high concentration of IL-6 standard and diluted with the assay diluent to produce samples with values within the dynamic range 0-200 pg ml^{-1}. The lower limit of detection (LLD, 3STD) of IL-6 was determined to be 0.39 pg ml^{-1} for dendrimer plate and 0.78 pg ml^{-1} for kit plate. The assay result showed good linearity within a dynamic range of assay and comparable to kit plate (Table 2). Serial dilutions did not affect the sensitivity or accuracy. These values demonstrate that dendrimer plate can be used to quantify the amount of IL-6 in serum samples and more sensitive than the kit plate. Consequently, the dendrimer plate was evaluated on real serum samples and the results were compared with kit plate. Five clinically acquired human serum samples with varying IL-6 and IL-1β concentration were tested, and the results are listed in Table 3. The serum samples from normal non-pregnant woman showed low levels of IL-6 as expected. However, pyelonephritis patients (pregnant) showed elevated levels of IL-6 and IL-1β, with comparable IL-6 levels. This suggests that, even though the blood cultures were positive for bacterial infection in patient 1, and negative for patient 2, the cytokines levels are already elevated due to pyelonephritis (an ascending urinary tract infection). The reasons from why IL-1β is more elevated in patient 1 than patient 2 are not known. The data from the dendrimer-plate and the kit plate were comparable. Therefore, dendrimer based sensors can provide sensitive assay for biomarkers diagnosis in clinically relevant samples.

The linear regression equation for dendrimer plate for IL-1β was $A = 0.04 + 0.007 * C_{[IL\text{-}1\beta]}$, with the linear regression coefficient R = 0.996. The lower limit of detection (LLD, 3STD) of IL-1β was determined to be 1.15 pg ml^{-1} for dendrimer plate, 2.08 pg ml^{-1} for kit plate and 3.93 pg ml-1 for physical adsorption (Table 4). Dendrimer modified plate showed 2 fold and 4 fold improvement on the detection limit compare to kit plate and physical adsorption respectively. Because IL-1β was a proof-of-concept study, we did not attempt luminol detection, which resulted in a 10-fold improvement in sensitivity for IL-6. These result suggested that the developed dendrimer based assay method can be applied to different cytokines and provide sensitive assay. Even though the dendrimer-modified plate is very stable, in the present form, where TMB or luminol detection is used, these assays are not meant to be reused.

3. Conclusions

We have developed a dendrimer-based capture strategy for biomarker detection, and have validated it by using it as a solid phase for IL-6 and IL-1β detection. IL-6 and IL-1β are important cytokines in a variety of inflammatory diseases, and are marker for chorioaminionitis. Hydroxyl/thiol functionalized G4-PAMAM dendrimers were covalently-immobilized onto maleimide- terminated PEG on a polystyrene plate by chemoselective coupling of the corresponding thiol and maleimide functional groups. Simultaneously, parts of the thiol groups on the dendrimer were converted to hydrazide groups by attaching maleimide and hydrazide-terminated bifunctional linker. The resulting dendrimer modified

surface is capable of binding capture antibody with favorable orientation of the antigen binding sites toward analyte phase by coupling of the hydrazide groups of dendrimer and aldehyde groups of oxidized antibody for effective binding of cytokines compared to equivalent phases prepared using the same antibody but immobilized by conventional method. The use of hydroxyl functionalized dendrimer and appropriate level of PEG on the plate suppress non-specific binding of proteins. The use of a long PEG linker and dendrimer between capture antibody and plate gives diffusional and conformational flexibility to the antibody for improved cytokine binding. The dendrimer-based capture of IL-6 shows a detection limit of 0.29 pg ml^{-1} for TMB detection and 0.13 pg ml^{-1} for luminol detection, both of which are significantly better than the commercial ELISA kit for IL-6. The LLD of IL-1β is 1.15 pg ml^{-1} which is more sensitive than the ELISA kit for IL-1β. The low detection limit of dendrimer-based plate suggests that conjugation reaction did not affect immunoreactivity of antibody. The dendrimer-based assays were validated using human serum samples from normal (non-pregnant) woman, and two pyelonephritis patients (pregnant women). The specificity and the improved sensitivity of the dendrimer-based *capture* strategy could have significant implications for the detection of a wide range of cytokines and biomarkers. Our current effort is aimed at improved *detection* methods, with a view to develop ELISA assays that are significantly better than conventional assays for *in situ* detection of inflammatory cytokines in the amniotic fluid. Early detection, followed by targeted therapy for neuroinflammation may lead to improved therapeutic outcomes for newborns with cerebral palsy.[54,55]

4. Experimental

Materials and Measurements

General reagents were purchased from Sigma-Aldrich. G(4)-PAMAM dendrimer was purchased from Dendritech®, Inc.(Midland, MI). DMSO-d_6 was purchased from Cambridge Isotope Laboratories. LC-SPDP, EMCH, SuperSignal ELISA Femto Maximum Sensitivity Substrate (37074), BCA Protein Assay Kit (23227), NAb Protein G Spin Kit (89949) and Gentle Ag/Ab binding and Elution Buffers (21027, 21020) were purchased from Pierce. Monoclonal IL-6 and IL-1β anti-human antibody, recombinant human IL-6 and IL-1β, biotinylated anti-human IL-6, and IL-1β antibody, streptavidin-HRP (DY998), reagent diluent(DY995), substrate reagent (TMB, DY999), stop solution (DY994) and wash buffer (WA126) were purchased from R&D Systems. and All MALDI-MS reference standards were purchased from Sigma-Aldrich. Matrix assisted laser desorption ionization (MALDI) mass spectra were acquired using a Bruker Ultraflex time-of-flight mass spectrometer. Spectra of all the functionalized dendrimers were obtained using a trans-3-indoleacrylic acid matrix with a matrix-analyte ratio of 3000:1 or 1000:1. Cytochrome C (MW 12,361 g mol^{-1}), and Trypsinogen (MW 23,982 g mol^{-1}) were used as external standards. An aliquot corresponding to 12-15 pmol of the analyte was deposited on the laser target. Positive ion mass spectra were acquired in linear mode. All data processing was performed using Bruker Daltonics flexAnalysis software. ^{1}H NMR spectra were recorded on Varian Mercury (400 MHz) spectrometers. Chemical shifts are reported in ppm from tetramethylsilane with the residual protic solvent resonance as the internal standard.

Atomic Force Microscopy (AFM)

AFM imaging was conducted using a Nanoscope III MultiMode atomic force microscope from Digital Instruments with an E-scanner (maximum scanning size 14.2×14.2 μm^2). For PEG and dendrimer modified ELISA plates, tapping mode in air was conducted by using silicon tips (TESP, VEECO). For the antibody-dendrimer modified ELISA plates, tapping mode was utilized in liquid cell (PBS, pH 7.4) by using silicon nitride probes (NP type, VEECO). The scan rate used was in the range of 1-2 Hz depending on the scan size. The images were taken with the area range from 500 × 500 nm^2 to 2 × 2 μm^2. The integral, and proportional gains used were approximately 0.4 and 0.7 respectively. All height images are reported and height images have been plane-fit in the fast scan direction with no additional filtering operation. The AFM images were analyzed using Nanoscope software version 5.12b by Veeco. The lateral dimension of a particle was determined at the full-width at half-maximum height in order to minimize tip convolution. For the bearing area analysis, the particle volume above the threshold plane is calculated by integrating the depth histogram over the entire area above the threshold plane. Roughness analysis was reported as the root-mean-square surface roughness $R_q = \sqrt{\sum \frac{z_i^2}{n}}$, where z_i is the height value and n is the number of the pixels in the image.

Synthesis of LC-PDP Functionalized G(4)-PAMAM Dendrimer 2

An methanol solution of amine terminated Starburst G(4)-PAMAM dendrimer (1.231 g of a 9.01% w/w solution in methanol, 111 mg, 7.8 μmole, MW 14215 g $mole^{-1}$) was evaporated to leave a foamy residue. The residue was dissolved in 4 ml DMF and 1 ml DMSO. To this solution 56 mg of LC-SPDP (132 μmole, 17 equiv.) in 1 ml DMSO and 30 mg (40 μl) of DIPEA (234 μmole, 30 equiv.) added. The reaction mixture was stirred for 15 hrs at room temperature under Ar. The reaction was quenched by adding 14 mg of acetic acid (234 μmole, 30 equiv.) in 3 ml of water. The reaction mixture was purified by dialysis against DMSO (MW cutoff 1k Da). The solution was lyophilized to give conjugate 2 as a yellow oily solid. The purified conjugate was characterized by ^{1}H NMR, HPLC and MALDI. The number of LC-PDP linker was determined by pyridine-2-thione assay as described in the manufacturer's protocol. Briefly, conjugate **2** was dissolved in PBS/EDTA buffer (pH 7.4, 1 mmole EDTA) and the absorbance was recorded at 343 nm in comparison to a PBS/EDTA blank. To this solution 10 μl of 15 mg ml^{-1} DTT was added and stirred for 15 min. After 15 min, the absorbance at 343 nm of the reduced sample was recorded (Fig. S10). The experiment was carried out in triplicate. On the basis of the change in absorbance, a molar ratio of 13 LC-PDP linkers per mole of dendrimer was calculated.

^{1}H NMR (400 MHz, DMSO-d_6, δ) 8.42 (d, 1H, pyridyl H), 7.92 (bs, amide NHs), 7.83 (bs, amide NHs), 7.79 and 7.73 (m, pyridyl Hs), 7.21(t, 1H, pyridyl H), 3.04-2.86 (bs,, m, 25H), 2.62-2.56 (bs, m, 18H), 2.47-2.39 (bs, 13H), 2.17 (bs, 16H) 2.01 (bt, 4H), 1.44 (m, 2.7H, PDP CH_2), 1.33 (m, 2.7H, PDP CH_2), 1.18 (m, 2.7H, PDP CH_2) ppm. MALDI-TOF (pos) *m/z* 18545.

Estimation of number of LC-PDP linker by MALDI. The MW of unfunctionalized G(4)-PAMAM-NH_2 dendrimer was determined to be 14159 g mol^{-1} by MALDI-TOF MS.

MALDI-TOF MS spectra was obtained after addition of LC-SPDP and change in MW upon LC-SPDP addition was divided by the Mw of LC-PDP (310.10 g $mole^{-1}$) to estimate number of LC-PDP linker.

$$Number\ of\ LCPDP\ linker = \frac{Mw(after\ LCSPDP\ addition)\ Mw\ G(4)PAMAM}{310.10} = \frac{1854514159}{310.10} = 13$$

Synthesis of LC-PDP/hydroxyl functionalized G(4)-PAMAM dendrimer 3

122 mg of conjugate **2** (6.4 μmole) was dissolved in 5 ml DMSO. To this solution 42 mg of 4-isothiocyanato-1-butanol **1** (322 μmole, 50 equiv.) was added. The reaction mixture was stirred for 24 hrs at room temperature. After 24 hrs, additional 25.2 mg of **1** (193.5 μmole, 30 equiv.) was added and allowed to react for an additional 24 hrs. The reaction mixture was purified by dialysis against DMSO (MW cutoff 1k Da). The solution was lyophilized to give **3** as a pale yellow oily solid.

^{1}H NMR (400 MHz, DMSO-d_6, δ) 8.42 (d, 1H, pyridyl H), 8.03 (bs, amide NHs), 7.92 (bs, amide NHs), 7.82-7.72 (bs, m, amide NHs, pyridyl Hs) 7.55 and 7.43 (bs, bs, 2.9H, $CH_2NHC(S)NHCH_2$), 7.21 (t, 0.48H, pyridyl H), 3.38 (t), 3.15 and 3.05 (bs, bs), 2.63 (bs, 11.3H), 2.41 (bs), 2.18(bs, 11.4H), 2.01(bt, 3.7H), 1.46-1.32 (m, 10.6 H), 1.18 (m, 2.4H) ppm. MALDI-TOF (pos) *m/z* 24642

ELISA Plate modification with PEG

230μl of EDC (3.4 μg, 17.8 nmole /well) and HOBT (2.7μg, 17.8 nmole/well) solution in pH 6.5 MES buffer was added to 96 well ELISA plate (Corning® high bind plate). 10μl of NH_2-PEG-Mel (MW 3.4k Da) (25 pg, 7.4 pmole/well) in pH 6.5 MES buffer was added to each well and incubated 30 min. at room temperature. 30μl of NH_2-PEG-OH (MW 2K) (10 mg, 5μmole/well) in MES buffer pH 6.5 was added to each well and incubated 8 hrs at room temperature. ELISA plate was washed with PBS (pH 7.4) and DI water, dried under N_2 stream and stored at -20°C.

Immobilization of dendrimer 3 to PEG layer

The following procedure was performed inside of glove bag. 2.2 mg of dendrimer conjugate **3** (98 nmole) was dissolved in 1ml of PBS/EDTA buffer (pH 7.4, 1mmole EDTA). To this solution, 0.84 mg of TCEP (2.94 μmole, 30 equiv.) was added. The reaction mixture was evacuated, flushed with N_2 and the reaction flask was transferred to inside of glove bag. The reaction mixture was stirred at room temperature under N_2 until all the conjugate **3** was dissolved and converted to free thiolated conjugate **4**. The glove bag was moved to cold room (4°C) and 7 μl of reaction mixture was diluted to 26 ml with PBS buffer and 260 μl of diluted reaction mixture (2.973 pmole of dendrimer conjugate **4** per well) was added to each well of PEG modified ELISA plate. To this ELISA plate, 10 μl of EMCH (44.595 pmole per well, 15 equiv.) in PBS buffer was added to each well and the ELISA plate was incubated for 3 hrs at 4 °C under constant N_2 flow. 3 μl of 2-mercaptoethanol was added to each well and incubated 1 hr. ELISA plate was washed with PBS (pH 7.4) and DI water, dried under N_2 stream and stored at -20°C.

Oxidation of anti-human IL-6 and IL-1β antibody and immobilization of antibody to dendrimer modified ELISA plate

1 mg of purified IL-6 or IL-1β antibody was reconstituted with 1 ml PBS (pH 7) at 4°C. 0.1 mg of $NaIO_4$ (5 μg $NaIO_4$ per 50 μg antibody) dissolved in 100 μl PBS (pH 7) was added to antibody solution and incubated 15 min. at 4°C (protected from light). Antibody solution was transfer to Amicon centrifuge filter tube (MW cut off 10k) and centrifuged 10 min. at 4°C (3000G). Concentrated antibody solution was diluted to 1ml with PBS buffer (pH 7.4), loaded to PD-10 column (pre equilibrated with pH 8 PBS) and centrifuged 2 min. at 1000G. The eluent was diluted to 29 ml with PBS buffer (pH 8) and 270 μl of diluted antibody solution was added to each well of dendrimer modified ELISA plate. The ELISA plate was incubated 3 hr at 4°C. 10 μl of $NaCNBH_3$ in PBS buffer (pH 8, 1mg $NaCNBH_3$/ml) was added to each well and incubated 3 hr at 4 °C. 5 μl of ethanolamine in PBS buffer (pH 7.4, 1μl ethanolamine/ml) was added to each well and incubated 1hr at 4 °C. Antibody immobilized ELISA plate was washed with wash buffer (R&D systems), added 300 μl of reagent diluents (R&D systems) stored at 4 °C overnight and performed assay.

General Procedure of ELISA Assay

The ELISA plate were washed with wash buffer four times (300 μl per well). 100 μl of each dilutions of IL-6 or IL-1β standard (300-0 pg ml^{-1}, two fold dilution) in reagent diluents were added to each well and incubated 2hr at room temperature. The each well of plate was washed five times with 300 μl of wash buffer. 10 μg of biotinylated anti-human IL-6 or IL-1β antibody was reconstituted with 10 ml of reagent diluent. 100 μl of reconstituted biotinylated anti-human IL-6 or IL-1β antibody solution was added to each well and incubated 2 hr at room temperature. The plate was washed again and 100 μl of streptavidin-horseradish peroxidase conjugate diluted 1:200 with reagent diluent was added to each well. The plate was incubated for 30 min. and washed again with wash buffer. 100 μl of substrate solution (TMB) was added to each well and incubated 30 min in the dark. Without washing the plate, 50 μl of stop solution (2N sulfuric acid) was added to each well to stop the color reaction. The absorbance was read immediately on a plate reader (Molecular Devices, SpectraMax M2) at 450 and 570 nm. For Luminol detection, 100 μl of SuperSignal ELISA Femto Maximum Sensitivity Substrate (37074) working solution according to manufacture's protocol added to each well. The plate was mixed for 1 minute using microplate mixer. The relative light units were measured at 425 nm using plate reader (Molecular Devices, SpectraMax M2) with luminescence setting.

Collection of human serum samples from pregnant women

We compared the performance of the ELISA and Dendrimer assays in the determination of serum IL-6 and IL-1β concentrations in two pregnant women with pyelonephritis, a condition frequently associated with a maternal systemic inflammatory response. Pyelonephritis was diagnosed in the presence of fever (temperature ≥38°C), clinical signs of an upper urinary tract infection (e.g., flank pain, costovertebral angle tenderness), pyuria, and a positive urine culture for microorganisms. Blood cultures were also obtained. Maternal serum samples were obtained by venipuncture at a similar gestational age (26.9 and 26.0 weeks of gestation), centrifuged at 1300 × g for 10 minutes at 4°C and stored at

-70°C until assay. Both patients provided written informed consent prior to the collection of maternal blood samples. The utilization of samples for research purposes was approved by the Institutional Review Boards of Wayne State University, and the National Institute of Child Health and Human Development (NICHD/NIH/DHHS). These samples have been employed to study the biology of inflammation, hemostasis, angiogenesis regulation, and growth factor concentrations during pregnancy. Patient 1 had a positive urine and blood culture for bacteria, while patient 2 had a positive urine culture for bacteria, but a negative blood culture. The maternal serum concentrations of IL-6 and IL-1β determined by ELISA and Dendrimer assays are displayed in Table 3.

Supplementary Material

Refer to Web version on PubMed Central for supplementary material.

Acknowledgments

This study was supported by the Intramural Research Program of the National Institute of Child Health and Human Development, NIH, DHHS.

References

1. Liu Z, Amiridis MD. J Phys Chem B. 2005; 109:16866. [PubMed: 16853146]
2. Stamatin I, Berlic C, Vaseashta A. Thin solid Films. 2006; 495:312.
3. a) Ajikumar PK, Ng JK, Tang YC, Lee JY, Stephanopoulos G, Too H-P. Langmuir. 2007; 23:5670. [PubMed: 17388617] b) Butler JE. Methods. 2000; 22:4. [PubMed: 11020313]
4. Yoon HC, Hong M-Y, Kim H-S. Anal Biochem. 2000; 282:121. [PubMed: 10860508]
5. Cobbe S, Connolly S, Ryan D, Nagde DL, Eritja R, Fitzmaurice D. J Phys Chem B. 2003; 107:470.
6. Salazer RB, Shovsky A, Schönherr H, Vancso GJ. Small. 2006; 2:1274. [PubMed: 17192974]
7. a) Benters R, Niemeyer CM, Drutschmann D, Blohm D, Wöhrle D. Nucleic Acid Research. 2002; 30:e10.b) Benters R, Niemeyer CM, Wöhrle D. CHEMBIOCHEM. 2001; 2:686. [PubMed: 11828505] c) Degenhart GH, Dordi B, Schönherr H, Vancso GJ. Langmuir. 2004; 20:6216. [PubMed: 15248705] d) Le Berre V, Trévisiol E, Dagkessamanskaia A, Sokol S, Caminade A-M, Majoral JP, Meunier B, François J. Nucleic Acid Research. 2003; 31:e88.
8. a) Selvaraju T, Das J, Han SW. Biosensors Bioelectronics. 2008; 23:932. [PubMed: 17977708] b) Liang K, Mu W, Huang M, Yu Z, Lai Q. Electroanalysis. 2006; 18:1505.
9. a) Zhu Y, Zhu H, Yang X, Xu L, Li C. Electroanalysis. 2007; 19:698.b) Bustos, Ma; Jiménez, GG.; Díaz-Sánchez, BR.; Juaristi, E.; Chapmam, TW.; Godínez, LA. Talanta. 2007; 72:1592.c) Xu L, Zhu Y, Tang L, Yang X, Li C. Electroanalysis. 2007; 19:717.
10. a) Yoon HC, Hong M-Y, Kim H-S. Langmuir. 2001; 17:1234.b) Yoon HC, Lee D, Kim H-S. Anal Chim Acta. 2002; 456:209.
11. Hong M-Y, Lee D, Kim H-S. Ananl Chem. 2005; 77:7326.
12. a) Jung LS, Campbell CT. J Phys Chem B. 2000; 104:11168.b) Jung LS, Campbell CT. Phys Rev Lett. 2000; 84:5164. [PubMed: 10990893]
13. a) Hong M-Y, Yoon HC, Kim H-S. Langmuir. 2003; 19:416.b) Hong M-Y, Kim Y-J, Lee JW, Kim K, Lee J-H, Yoo J-S, Bae S-H, Choi B-S, Kim H-S. J Colloid Interface Sci. 2004; 274:41. [PubMed: 15120276]
14. Park S, Lee K-B, Choi IS, Langer R, Jon S. Langmuir. 2007; 23:10902. [PubMed: 17900199]
15. a) Park J, Kurosawa S, Takai M, Ishihara K. Collids and Surfaces. 2007; 55:164.b) Chapman RG, Ostuni E, Takayama S, Holmlin RE, Yan L, Whitesides GM. J Am Chem Soc. 2000; 122:8303.c) Unsworth LD, Sheardown H, Brash JL. Langmuir. 2005; 21:1036. [PubMed: 15667186] d) Huang

N-P, Vörös J, De Paul SM, Textor M, Spencer ND. Langmuir. 2002; 18:220.e) Herrwerth S, Feng RC, Fick J, Eck W, Himmelhaus M, Dahint R, Grunze M. Langmuir. 2003; 19:1880.

16. a) Prime KL, Whitesides GM. Science. 1991; 252:1164. [PubMed: 2031186] b) Vanderah DJ, La H, Naff J, Silin V, Rubinson KA. J Am Chem Soc. 2004; 126:13639. [PubMed: 15493920] c) Unsworth LD, Sheardown H, Brash JL. Langmuir. 2008; 24:1924. [PubMed: 18217777]
17. a) Rüetschi U, Rosén Å, Karlsson G, Zetterberg H, Rymo L, Hagberg H, Jacobsson B. J Proteome Res. 2005; 4:2236. [PubMed: 16335971] b) Slattery MM, Morrison JJ. Lancet. 2002; 360:1489. [PubMed: 12433531]
18. Gotsch F, Kusanovic JP, Mazaki-Tovi S, Pineles BL, Erez O, Espinoza J, Hassan SS. Clin Obstet Gynecol. 2007; 50:652. [PubMed: 17762416]
19. a) Romero R, Sirtori M, Oyarzun E, Avila C, Mazor M, Callahan R. Am J Obstet Gynecol. 1989; 161:817. [PubMed: 2675611] b) Harirah H, Donia SE, Hsu C-D. Obstet Gynecol. 2002; 99:80. [PubMed: 11777515]
20. a) Romero R, Mazor M. Clin Obstet Gynecol. 1988; 31:553. [PubMed: 3066544] b) Romero R, Espinoza J, Gonçalves LF, Kusanovic JP, Friel LA, Nien JK. Semin Fetal & Neonatal Med. 2006; 11:317. [PubMed: 16839830] c) Romero R, Chaiworapongsa T, Espinoza JJ. Netrition. 2003; 133:1688S.
21. Romero R, Gotsch F, Pineles B, Kusanovic JP. Neutri Rev. 2007; 65:S194.
22. a) Messina GA, Panini NV, Martinez NA, Raba J. Anal Biochem. 2008; 380:262. [PubMed: 18577366] b) Naugler W, Karin M. Trends Molecular Med. 2008; 14:109.
23. Gomez R, Romero R, Ghezzi F, Yoon BH, Mazor M, Berry SM. Am J Obstet Gynecol. 1998; 179:194. [PubMed: 9704787]
24. a) Ottaviani MF, Jockusch S, Turro N, Tomalia DA, Barbon A. Langmuir. 2004; 20:10238. [PubMed: 15518519] b) Klajnert B, Stanisławska L, Bryszewska M, Pałecz B. Biochim Biophys Acta. 2003; 1648:115. [PubMed: 12758154] c) Gabellieri E, Strambini GB, Shcharbin D, Klajnert B, Bryszewska M. Biochim Biophys Acta. 2006; 1764:1750. [PubMed: 17055349]
25. a) Burns JA, Butler JC, Moran J, Whitesides GM. J Org Chem. 1991; 56:2648.b) Getz EB, Xiao M, Chakrabarty T, Cook R, Selvin PR. Anal Biochem. 1999; a:73. [PubMed: 10452801]
26. a) Shimo T, Matsuda Y, Iwanaga T, Shinmyozu T, Somekawa K. Heterocycles. 2007; 71:1053.b) Hahn H-G, Nam KD, Mah H. Heterocycles. 2001; 55:1238.
27. Yam CM, Deluge M, Tang D, Kumar A, Cai C. J Colloid Interface Sci. 2006; 296:118. [PubMed: 16226763]
28. Nagasaki Y, Kobayashi H, Katsuyama Y, Jomura T, Sakura T. J Colloid Interface Sci. 2007; 309:524. [PubMed: 17368469]
29. a) Schramm W, Paek S-H, Voss G. Immunomethods. 1993; 3:93.b) Rebeski DE, Winger EM, Shin Y-K, Lelenta M, Robinson MM, Varecka R, Crowther JR. J Immuno Method. 1999; 226:85.
30. Lynch M, Mosher C, Huff J, Nettikadan S, Johnson J, Henderson E. Proteomics. 2004; 4:1695. [PubMed: 15174138]
31. a) Singh P. Biotechnol Appl Biochem. 2007; 48:1. [PubMed: 17688425] b) Tokuhisa H, Liu J, Omori K, Kanesato M, Hiratani K, Baker LA. Langmuir. 2009; 25:1633. [PubMed: 19117477]
32. Nie T, Baldwin A, Yamaguchi N, Kiick K. J Controlled Release. 2007; 122:287.
33. a) Heyes CD, Groll J, Möller M, Nienhaus U. Mol Biosyst. 2007; 3:419. [PubMed: 17533455] b) Sofia SJ, Premnath V, Merrill EW. Macromolecules. 1998; 31:5059. [PubMed: 9680446]
34. Bhat R, Timasheff SN. Protein Sci. 1992; 1:1133. [PubMed: 1304392]
35. Choi J-W, Chun BS, Oh B-K, Lee W, Lee WH. Coll Surf B: Biointerfaces. 2005; 40:173.
36. Jung Y, Kang HJ, Lee JM, Jung SO, Yun WS, Chung SJ, Chung BH. Anal Biochem. 2008; 374:99. [PubMed: 18023402]
37. a) Snopok B, Yurchenko M, Szekely L, Klein G, Kashuba E. Anal Bioanal Chem. 2006; 386:2063. [PubMed: 17086389] b) Turiel E, Fernández P, Pérez-Conde C, Gutiérrez AM, Cámara C. Fresenius J Anal Chem. 1999; 365:658.c) Ahmed SR, Lutes AT, Barbari TA. J Membrane Sci. 2006; 282:311.
38. a) Fowler JM, Stuart MC, Wong DKY. Ananl Chem. 2007; 79:350.b) Jung Y, Lee JM, Jung H, Chung BH. Anal Chem. 2007; 79:6534. [PubMed: 17668928]

39. Jung Y, Jeong JY, Chung BH. Analyst. 2008; 133:697. [PubMed: 18493668]
40. Peluso P, Wilson DS, Do D, Tran H, Venkatasubbaiah M, Quincy D, Heidecker B, Poindexter K, Tolani N, Phelan M, Witte K, Jung LS, Wagner P, Nock S. Ananl Biochem. 2003; 312:113.
41. Leibiger H, Wüstner D, Stigler R-D, Marx U. Biochem J. 1999; 338:529. [PubMed: 10024532]
42. Coco-Martin JM, Brunink F, van der Velden-de Groot TAM, Beuvery EC. J Immunological Methods. 1992; 155:241. [PubMed: 1431152]
43. Qian J, Liu T, Yang L, Daus A, Crowley R, Zhou Q. Anal Biochem. 2007; 364:8. [PubMed: 17362871]
44. Rademacher TW, Homans SW, Parekh RB, Dwek RA. Biochem Soc Symp. 1986; 51:131. [PubMed: 3814165]
45. Liu H, Gaza-Bulseco G, Faldu D, Chumsae C, Sun J. J Pharmaceutical Sci. 2008; 97:2426.
46. a) Abraham R, Moller D, Gabel D, Senter P, Hellström I, Hellström KE. J Immunological methods. 1991; 144:77. [PubMed: 1660058] b) Wolfe CAC, Hage DS. Anal Biochem. 1995; 231:123. [PubMed: 8678290]
47. a) Singh, P.; Moll, F., III; Cronin, P.; Lin, H.; Ferzli, C.; Koski, K.; Saul, R. U S Patent. 5898005. 1999. b) Jacobsen NW, Dickinson RG. Anal Chem. 1974; 46:298.
48. Roberts JC, Adams YE, Tomalia D, Mercer-Smith JA, Lavallee DK. Bioconjugate Chem. 1990; 1:305.
49. Fischer-Durand N, Salmain M, Rudolf B, Vessières A, Zakrzewski J, Jaouen G. ChemBioChem. 2004; 5:519. [PubMed: 15185376]
50. a) Wan L, Manickam DS, Oupicky D, Mao G. Langmuir. 2008; 24:12474. [PubMed: 18839970] b) Handa H, Gurczynski S, Jackson MP, Auner G, Walker J, Mao G. Surface Science. 2008; 602:1392. [PubMed: 19461940]
51. a) Li J, Piehler LT, Qin D, Baker JR Jr, Tomalia DA, Meier DJ. Langmuir. 2000; 16:5613.b) Abdelhady HG, Allen S, Davies MC, Roberts CJ, Tendler SJB, Williams PM. Surface Sci. 2004; 558:99.c) Hierlemann A, Campbell JK, Baker LA, Crooks RM, Ricco AJ. J Am Chem Soc. 1998; 120:5323.
52. Wang C, Zhang Y. Sensors and Actuators B. 2006; 120:125.
53. Berggren C, Bjarnason B, Johansson G. Biosensors & Bioelectronics. 1998; 13:1061. [PubMed: 9842701]
54. Navath R, Wang B, Kortoglu Y, Kannan S, Romero R, Kannan RM. Bioconjugate Chemistry. 2008; 19:2446. [PubMed: 19053299]
55. Kannan, R.; Kannan, S.; Romero, R.; Navath, R.; Dai, H.; Wang, B. Dendrimer based nanodevices for maternal fetal applications. US Provisional patent, application. 61187263. Jun. 2009

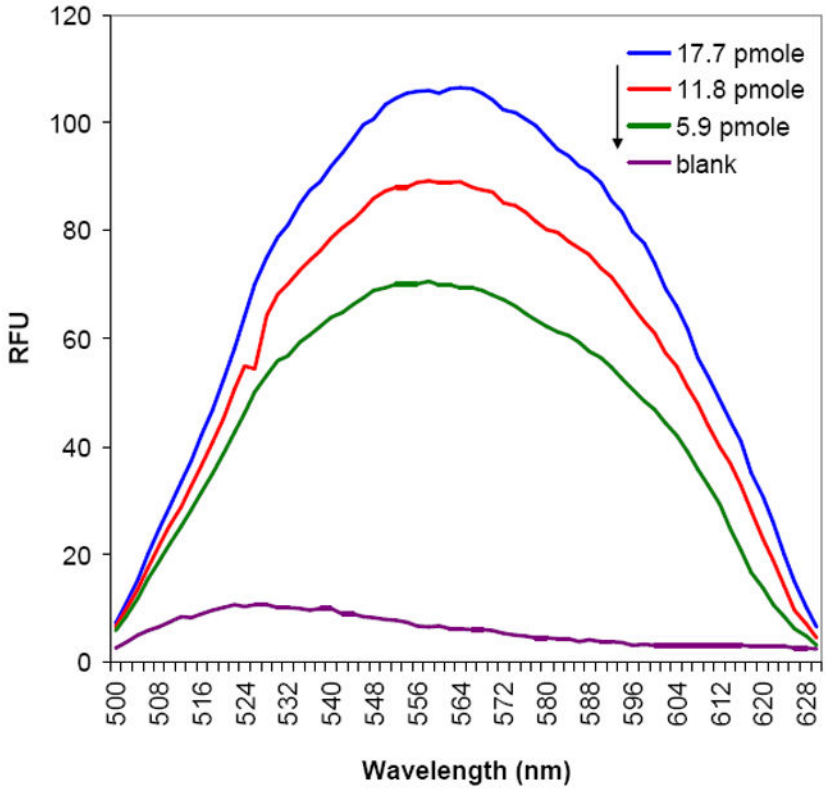

Figure 1.

Emission spectra of thiol/hydroxyl G4-PAMAM **4** and PyMPO immobilized ELISA plate in MeOH for different dendrimer concentration [Ex: 410 nm].

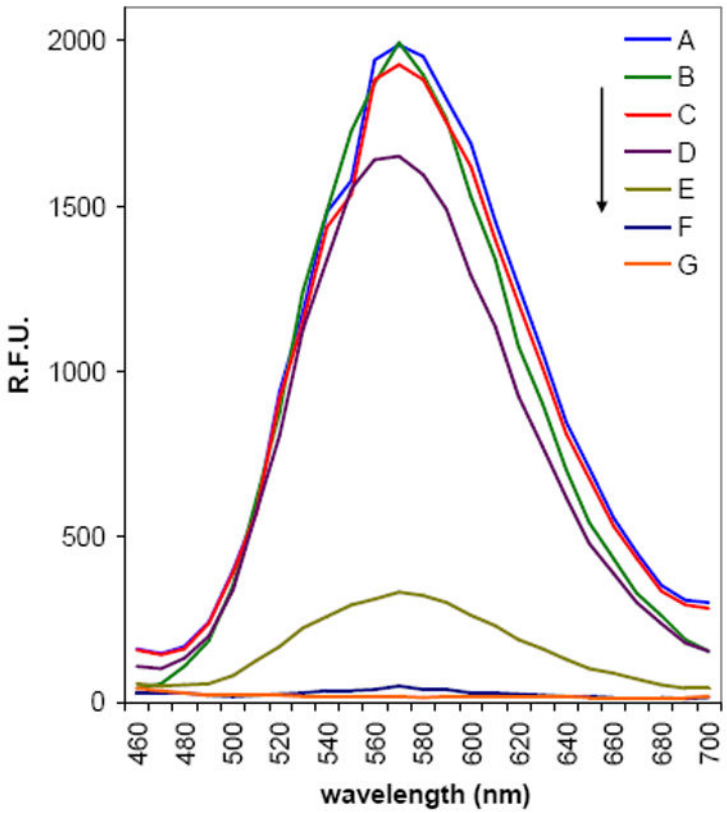

Figure 2.

Fluorescence intensity of antibody-dendrimer conjugate reaction mixture. [Ex: 410 nm in PBS pH 7.4] (A) Free dendrimer **6** (276 fM) before immunoprecipitation (IP). (B) Reaction mixture of antibody-dendrimer conjugation before IP. (C) Free dendrimer **6** after IP. (D) Reaction mixture of antibody-dendrimer conjugation after IP. (E) Eluted bound antibody-dendrimer conjugate, dendrimer **6** and antibody mixture. (F) Eluted nonspecifically adsorbed free dendrimer **6**. (G) Free antibody (50 μg ml^{-1}, 333 nM).

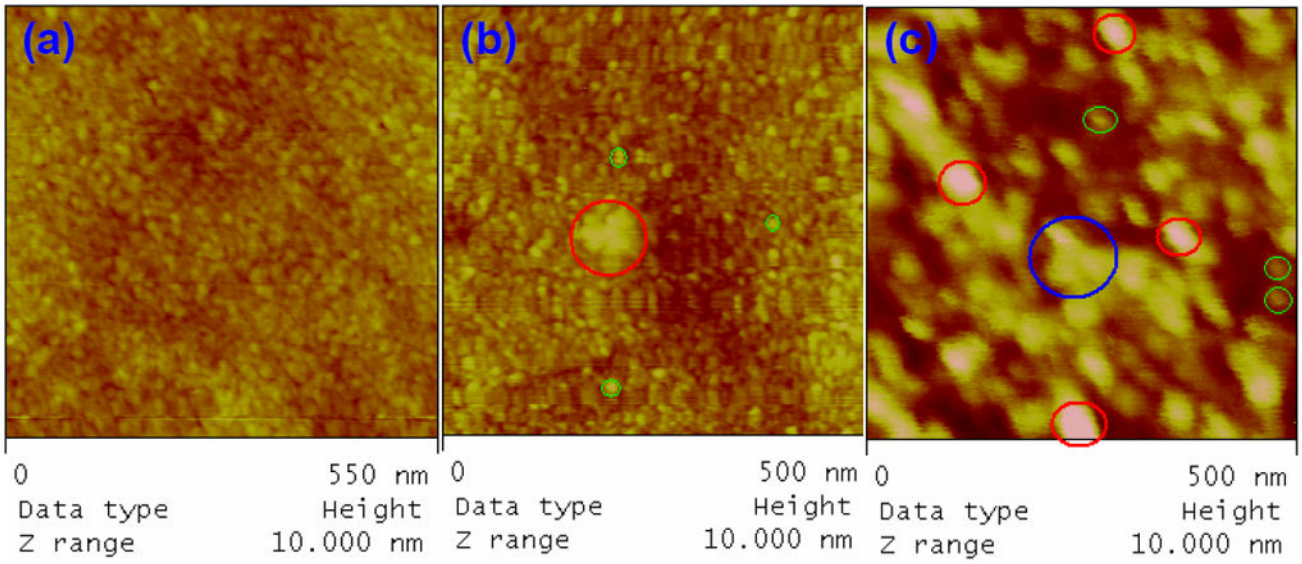

Figure 3.

(a) AFM height image of 2k PEG-OH and 3.4k PEG-Mal modified ELISA plate, conducted in air with the tapping mode. (b) AFM height image of dendrimer **4** attached on PEG modified substrate, conducted in air with the tapping mode. (c) A typical AFM height image of antibody-dendrimer conjugate attached on PEG modified ELISA plate. The image was conducted in tapping mode in liquid cell filled with PBS pH 7.4.

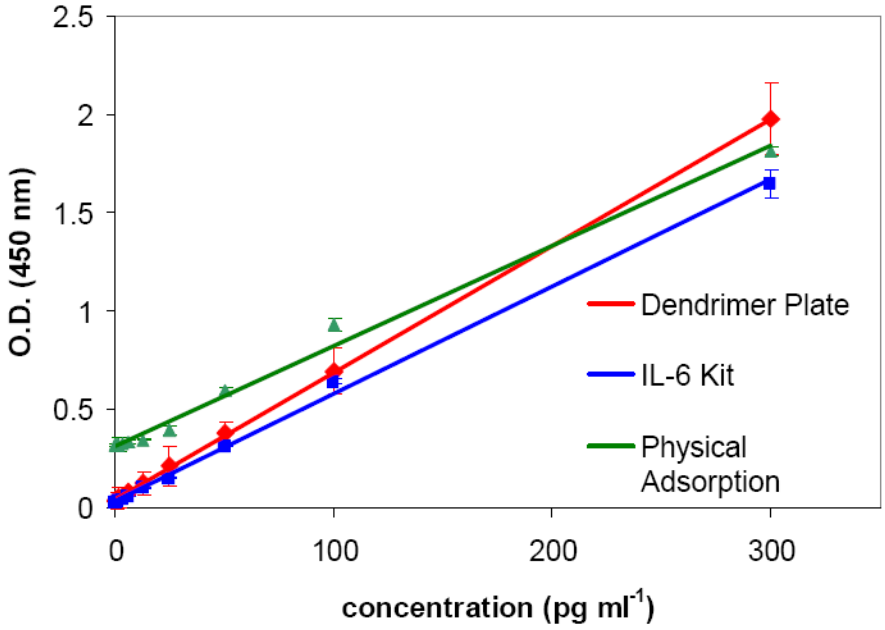

Figure 4.
Standard curves for IL-6 ELISA measured with the dendrimer plate, IL-6 kit and plate prepared by physical adsorption of anti-human IL-6 antibody.

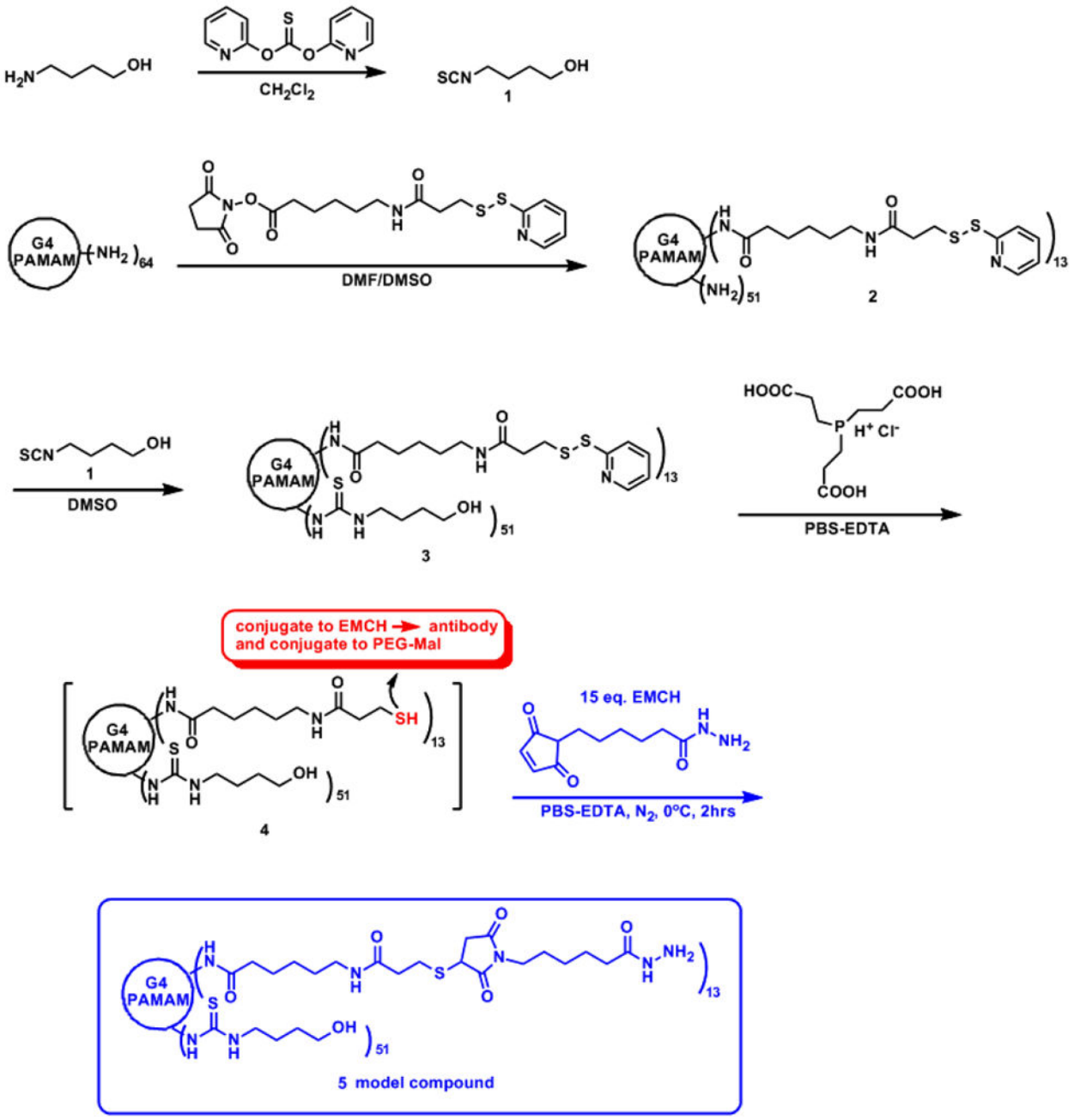

Scheme 1.

Synthesis of hydroxyl/LC-PDP conjugated G4-PAMAM dendrimer **4**.

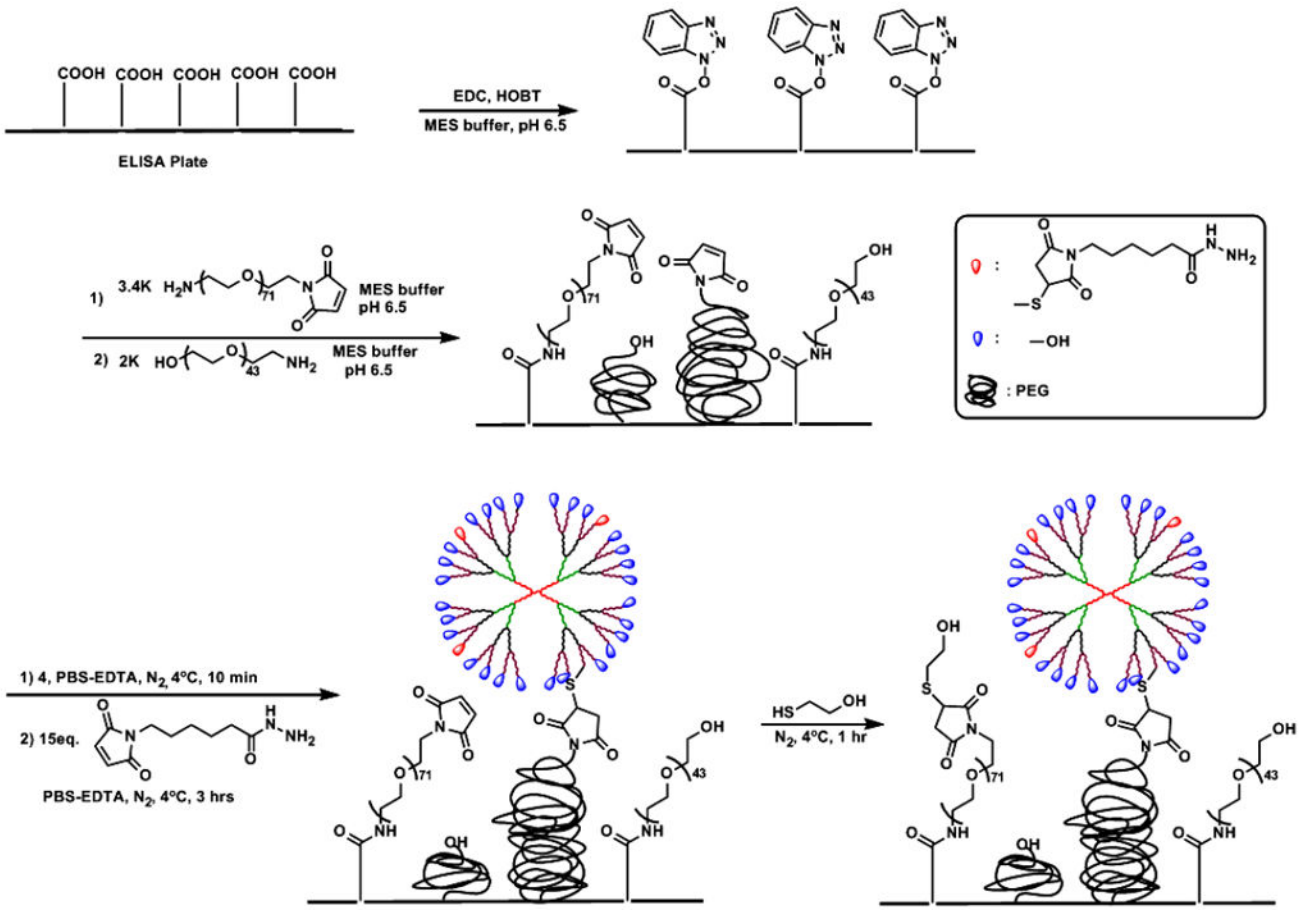

Scheme 2.

Schematic representation of ELISA plate modification with PEG and immobilization of hydroxyl/LC-PDP-G4 PAMAM **4** onto PEG layer.

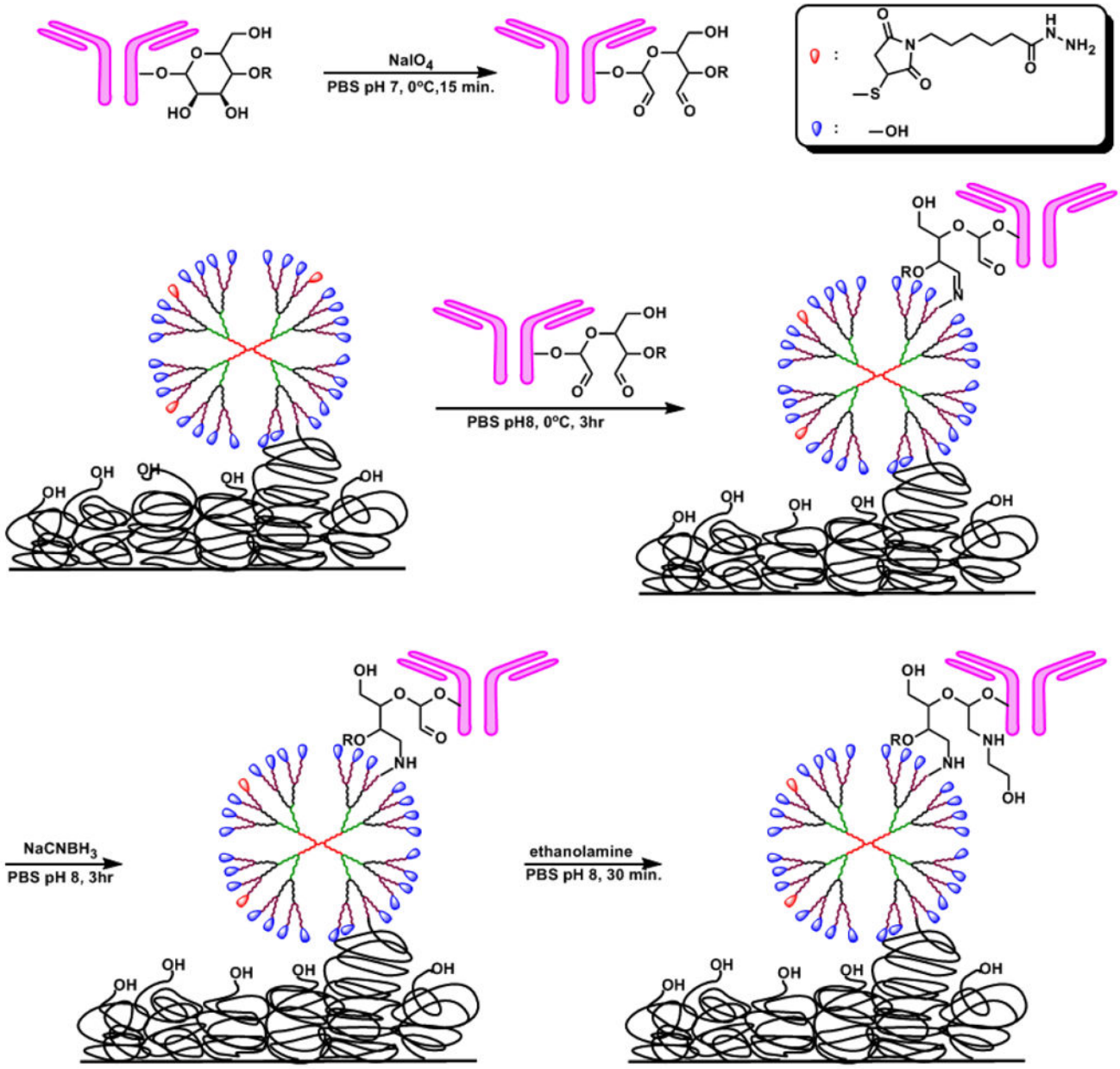

Scheme 3.
Schematic representation of antibody immobilization on to the dendrimer.

Table 1

IL-6 ELISA data obtained from dendrimer plate, kit plate, by physical adsorption and dendrimer plate with luminol detection.

concentration [pg ml^{-1}]	Dendrimer Plate TMB detection [O.D.]	IL-6 kit TMB detection [O.D.]	Physical Adsorption TMB detection [O.D.]	Dendrimer Plate Luminol detection [R.L.U.]
300	1.975	1.647	1.813	–
100	0.697	0.643	0.931	7420.6
25	0.213	0.151	0.395	3002.0
6.25	0.085	0.059	0.336	1831.8
1.56	0.05	0.035	0.323	1435.8
0.78	0.042	0.032	0.321	1331.5
0.39	0.038	–	0.322	1247.9
0.195	0.035	–	0.321	1226.1
0.098	–	–	–	1205.6
0	0.034	0.031	0.319	1109.6
STD, $[0]_{IL-6}$	0.00346	0.0025	0.009	33.4
RSD [%], $[0]_{IL-6}$	10.1	8.1	7.8	6.6
R^2	0.999	0.997	0.992	0.995
LLD[^{a}]	0.04438	0.0385	0.346	1209.7
Sensitivity [pg ml^{-1}]	< 0.29	< 0.87	< 5.75	< 0.13

*[a]*The lower limit of detection (LLD) of IL-6 was determined by adding three STD to the mean OD of five zero standard replicates and calculate the corresponding concentration from the standard curve.

Table 2

Comparison of serium IL-6 concentrations using two methods.[a]

	Dendrimer Plate			Kit Plate	
Dilution	**Expected [pg ml^{-1}]**	**Observed [pg ml^{-1}]**	**[%]** $\frac{Observed}{Expected}$	**Observed [pg ml^{-1}]**	**[%]** $\frac{Observed}{Expected}$
neat	200	193.9	97	193.5	96.8
1:2	100	96.1	96.1	109.4	109.4
1:4	50	59.2	118.4	53.1	106.2
1:8	25	27.2	108.8	25.4	101.6
1:16	12.5	12.1	96.8	12.1	96.8

[a]Human serum samples (from a non-pregnant woman) were spiked with high concentrations of IL-6 and diluted with assay diluent to produce samples with values within the dynamic range of the assay.

Table 3

Cytokine detection in human serum samples from normal non-pregnant and pregnant women with pyelonephritis, using the two methods.

Samples	Dendrimer Plate Concentration [pg ml^{-1}]	Kit Plate Concentration [pg ml^{-1}]
Normal non-pregnant women serum [IL-6]	1.48	1.51
Pyelonephritis Positive BC [IL-6] [Patient 1]	292	312
Pyelonephritis Negative BC [IL-6] [Patient 2]	252	215
Pyelonephritis Positive BC [IL-1β] [Patient 1]	809	[a]
Pyelonephritis Negative BC [IL-1β] [Patient 2]	303	[a]

[a] not measured.

BC: blood culture

Table 4

IL-1β ELISA data obtained from dendrimer plate, kit plate, by physical adsorption.

concentration [pg ml^{-1}]	Dendrimer Plate [O.D.]	IL-1β kit [O.D.]	Physical Adsorption [O.D.]
250	1.781	1.806	1.215
62.5	0.519	0.561	0.712
15.6	0.146	0.149	0.576
3.9	0.055	0.043	0.512
1.95	0.044	0.030	0.506
0.975	0.034	-	0.499
0	0.021	0.014	0.491
R^2	0.996	0.995	0.991
LLD	0.04	0.032	0.516
Sensitivity [pg ml^{-1}]	<1.15	<2.08	<3.93